Journal of Fluorine Chemistry 132 (2011) 244–249

Contents lists available at ScienceDirect

Journal of Fluorine Chemistry

journal homepage: www.elsevier.com/locate/fluor

^{115}In and ^{19}F MAS NMR study of $(NH_4)_3InF_6$ phases

G. Scholz [a,*], T. Krahl [b], M. Ahrens [a,1], C. Martineau [c,2], J.Y. Buzaré [c], C. Jäger [b], E. Kemnitz [a,*]

[a] Humboldt-Universität zu Berlin, Institut für Chemie, Brook-Taylor-Str. 2, D-12489 Berlin, Germany
[b] Bundesanstalt für Materialprüfung und –forschung, Richard-Willstätter-Straße 11, D-12489 Berlin, Germany
[c] Laboratoire de Physique de l'Etat Condensé (UMR CNRS 6087), Institut de Recherche en Ingénierie Moléculaire et Matériaux Fonctionnels (FR CNRS 2575), Université du Maine, Avenue O. Messiaen, 72085 Le Mans Cedex 9, France

ARTICLE INFO

Article history:
Received 7 December 2010
Received in revised form 17 January 2011
Accepted 21 January 2011
Available online 1 February 2011

Keywords:
$(NH_4)_3InF_6$
^{115}In and ^{19}F solid state NMR
XRD

ABSTRACT

This study presents for the first time an NMR spectroscopic characterization of the room and high temperature phases of $(NH_4)_3InF_6$ using ^{19}F and ^{115}In as probe nuclei. The reversible phase transition to the cubic phase at 353 K was followed by MAS NMR in situ. Static NMR experiments of the room temperature phase and MAS NMR experiments of the high temperature phase allowed the determination of the NMR parameters of both nuclei. Finally, the scalar In–F coupling, rarely observed in solid state NMR, is evidenced in both room and high temperature phases of $(NH_4)_3InF_6$, and measured in the high temperature phase.

1. Introduction

$(NH_4)_3InF_6$ is one of the numerous compounds belonging to the class of elpasolites with the common formula $M^I{}_2M^{I'}M^{III}F_6$ (M^I, $M^{I'}$ = Li, Na, K, Rb, Cs, Tl, Ag, NH_4, M^{III} = Al, Ga, In, Sc, Ti, V, Cr, Fe, Y, Ln). In general, these compounds exhibit cubic high-temperature phases and less symmetric structures at lower temperatures [1]. Phase transitions between these phases have been explained in terms of rotational reorientations of the $M^{III}F_6$ octahedra and NH_4 tetrahedra in the special case of ammonium ions as M^I ($M^{I'}$) [2,3]. Among ammonium elpasolites, the ones with small trivalent cations (M = Al, Ga, Cr, Fe) are best known. Phase transitions have been studied using X-ray diffraction and differential scanning calorimetry [4,5]. These compounds exhibit a cubic high-temperature phase ($Fm\bar{3}m$), which is stable at room temperature, a monoclinic low-temperature phase ($P2_1/n$).

In the high-temperature phases, the NH_4 tetrahedra occupying the $M^{I'}$ position are twofold disordered, the MF_6 octahedra are disordered up to eightfold. The phase transition between both phases is an order–disorder transition. NH_4 and MF_6 are fully ordered in the low temperature phase. The phase transition entropy ΔS is determined by the change in the number degrees of freedom W by $\Delta S = R \ln W$, which reach the maximum value $R \ln 16$ in the case of Ga and Fe [6].

$(NH_4)_3InF_6$ shows a more complex succession of phase transitions, analogous to $(NH_4)_3ScF_6$. The cubic high-temperature phase is stable above 352 K. The room-temperature phase is reported to be tetragonal [7] or monoclinic [8]. At least one additional phase transition to an intermediate phase is observed at 318 K, however, no change in the X-ray power diffraction diagram was observed at that temperature. The overall entropy difference between the high-temperature and room-temperature is around $R \ln 16$, hence the room-temperature phase must be ordered [5]. This result is inconsistent with the assumed tetragonal symmetry of this phase, requiring at least one twofold disordered ammonium ion. Another transition is observed at 230 K. The final symmetry at very low temperature is announced to be triclinic for all ammonium elpasolites [9], however, a monoclinic structure of $(NH_4)_3InF_6$ at 113 K has been reported recently [10].

Tetragonal symmetry was also reported for the room temperature phase of $(NH_4)_3ScF_6$ [7], which was later corrected to monoclinic symmetry [11]. The authors state explicitly that the symmetry of this monoclinic phase is close to tetragonal. Resolution can be only achieved with high resolution diffraction methods. For more clarity a schematic overview of the present knowledge on phases and phase transitions of $(NH_4)_3InF_6$ is given in Fig. 1.

Although local spectroscopic techniques like solid state NMR could contribute to solve the question concerning the existence of different indium and fluorine sites, so far, neither ^{19}F nor ^{115}In solid state NMR studies were reported for this compound. On the other hand, as shown for $(NH_4)_3GaF_6$ the application of solid state NMR is a valuable tool to obtain local spectroscopic information [12].

* Corresponding authors.
E-mail address: Gudrun.Scholz@rz.hu-berlin.de (G. Scholz).
[1] Current address: Fraunhofer Research Institution for Polymeric Materials and Composites PYCO, Kantstrasse 55, 14513 Teltow, Germany.
[2] Current Address: Tectospin – Institut Lavoisier de Versailles (UMR CNRS 8180), Université de Versailles Saint-Quentin en Yvelines, 45 Avenue des Etats-Unis, 78035 Versailles Cedex, France.

0022-1139/$ – see front matter © 2011 Elsevier B.V. All rights reserved.
doi:10.1016/j.jfluchem.2011.01.010

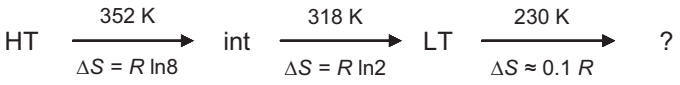

Fig. 1. Overview of the phase transitions of $(NH_4)_3InF_6$ (HT, high temperature phase; int, intermediate phase; LT, low temperature phase).

In principle, both nuclei forming the $(InF_6)^{3-}$ octahedra should be easily spectroscopically accessible, ^{19}F ($I = 1/2$) and ^{115}In ($I = 9/2$) have a sufficient natural abundance (Table 1). However, for ^{19}F NMR, the spectral resolution is often limited because of the strong homonuclear dipolar coupling, which is usually not averaged out at moderate MAS frequencies, leading to broad and only little structured ^{19}F NMR lines. Problems with Indium are less aligned with the second isotope ^{113}In but mainly with the large nuclear spin along with the large quadrupolar moment (Q), which is about 8 times larger than that of ^{71}Ga, the nucleus investigated in [12]. The quadrupolar moments of the indium isotopes are largest of all naturally occurring isotopes of the main group elements. Magnetic properties of the nuclei used as probes in this study are summarized in Table 1.

The strong quadrupolar moment of In combined with non-cubic symmetries of the crystals and together with the number of possible spin transitions result in indium NMR spectra mostly dominated by large quadrupolar interactions and difficult to acquire experimentally. A resolution by MAS is in general not possible applying conventional spinning frequencies up to 35 kHz.

These properties of the In isotopes are responsible for the situation that ^{115}In NMR measurements are very scarce in the literature. Usually these are static measurements as e.g. given for Na_3InCl_6 [13]. For Li_3InBr_6 [14] a characteristic signal was detectable only at higher temperatures ($T > 479$ K) for which the large quadrupolar interaction is partially averaged out by motional effects. Wasylishen et al. [15] investigated several indium complexes by static ^{115}In NMR measurements and determined quadrupolar coupling constants C_Q up to 200 MHz.

Table 1
Magnetic properties of fluorine and indium nuclei.

Property	^{19}F	^{115}In	^{113}In
I	1/2	9/2	9/2
Q (10^{-30} m^2)	0	81	79.9
Larmor frequency (MHz)[a]	376.5	87.7	87.5
Natural abundance (%)	100	95.7	4.3

[a] Magnetic field: 9.4 T.

The intention of the present study is an NMR spectroscopic characterization of the room temperature and high temperature phases of $(NH_4)_3InF_6$ using ^{19}F and ^{115}In as probe nuclei. For ^{115}In this is not only a challenge for the room temperature phase but the spectra were also never before observed for the cubic phase. The reversible phase transition to the cubic phase at 353 K has been followed by in situ MAS NMR. ^{115}In NMR spectra of the low temperature phase were recorded at different magnetic fields, allowing the determination of the number of indium sites and the measurement of their quadrupolar parameters.

In $(NH_4)_3GaF_6$ the scalar Ga–F-coupling was directly observed at room temperature in the cubic phase [12]. Using ^{19}F and ^{115}In decoupling the ^{19}F–^{115}In scalar coupling is directly evidenced and measured both on the ^{19}F MAS and on the ^{115}In MAS NMR spectra of the high-temperature phase. Synchrotron X-ray powder diffraction was carried out to support the evaluation of the NMR results.

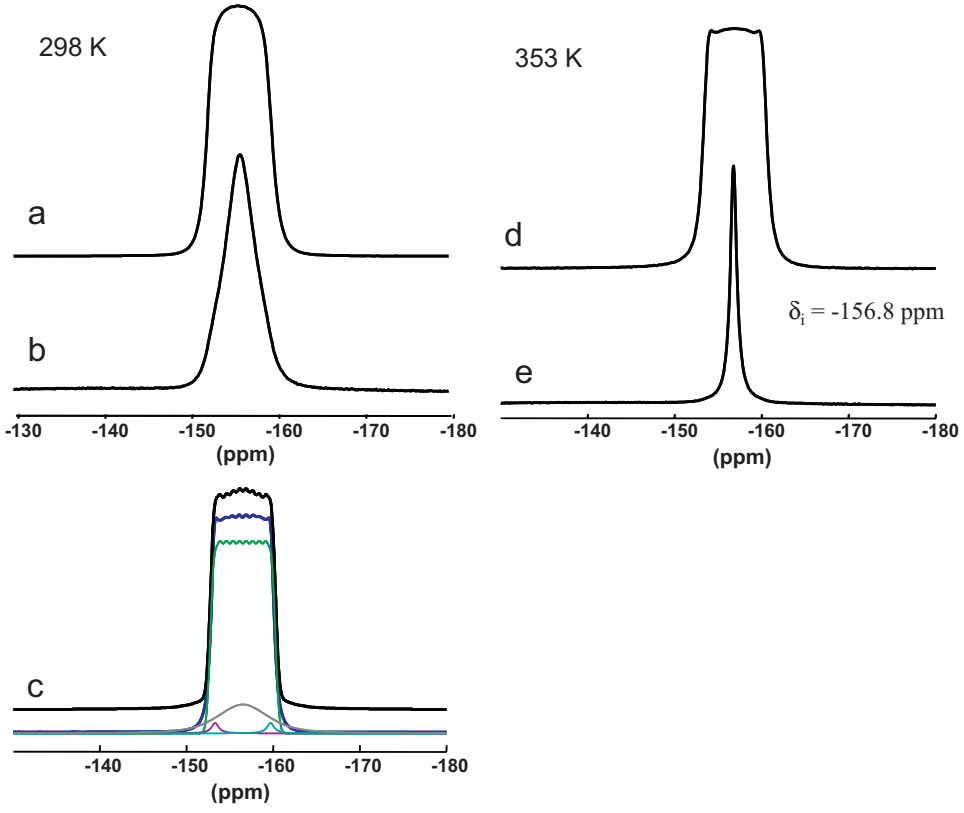

Fig. 2. ^{19}F MAS NMR spectra of $(NH_4)_3InF_6$ taken at 298 K (a–c)and 353 K (d and e): (a–e) single pulse MAS spectra; (a, b, d and e) $\nu_{rot} = 25$ kHz, (c) $\nu_{rot} = 34$ kHz, recorded at 9.4 T (blue) and 7 T (black); (b and e) ^{19}F–{^{115}In}-cw-decoupled MAS spectra. (For interpretation of the references to color in this figure legend, the reader is referred to the web version of the article.)

Table 2
NMR parameters obtained by simulation of the static ^{115}In NMR spectra of the room temperature phase of $(NH_4)_3InF_6$ recorded at three different magnetic fields (Fig. 3 A).

Line #	δ_{iso} (ppm)[a]	ν_Q (kHz)	η_Q	Relative intensity (%)
#1	−122	1428	0.92	55
#2	−122	2859	0.31	45

[a] d_{CS} = 10 ppm; η_{CS} = 1.0 for both sites.

Table 3
Reconstruction of the ^{19}F MAS NMR spectrum of the cubic phase of $(NH_4)_3InF_6$ recorded at 353 K (Fig. 2d).

Line #	δ_{iso} (ppm)	FWHM (kHz)	Relative intensity (%)
#1	−156.9 J = 284 Hz	0.60	97.0
#2	−153.7	0.38	1.1
#3	−160.2	0.38	1.9

2. Results

2.1. $(NH_4)_3InF_6$ – NMR at room temperature

The ^{19}F MAS NMR spectrum of $(NH_4)_3InF_6$ taken at 298 K has a very unusual line shape as shown in Fig. 2a. Residual ^{19}F homonuclear dipolar couplings and possible scalar couplings result in a broad NMR line (FWHM ~ 2.8 kHz) with a convex shape. Because of the lack of resolution, the number of fluorine sites can hardly be determined. However, the asymmetrical line shape of the ^{19}F resonance under ^{115}In decoupling (Fig. 2b) unequivocally indicates the presence of several sites.

Information about the room temperature phase from ^{115}In NMR spectra is hampered by the strong quadrupolar interaction of the In nuclei in non-cubic phases leading to very broad signals. They are too broad to be resolved by MAS NMR. For that reason static ^{115}In NMR spectra were recorded at 7.0 T, 9.4 T and 14.1 T. The resulting spectra are shown in Fig. 3A. As expected, the spectra are mostly governed by the effects of the second order of the ^{115}In large quadrupolar interactions, which are reduced as the magnetic field is increased (Fig. 3A). The central transition spans a region of about 12,000 ppm at the lowest field employed here (7.0 T).

The three ^{115}In NMR spectra can be reconstructed using a single set of parameters and two indium sites (Table 2).

2.2. $(NH_4)_3InF_6$ – NMR at 353 K (cubic phase)

Although only one fluorine site is expected in the high temperature cubic phase, the pattern of the ^{19}F MAS NMR spectrum is again particular but different from that of the room temperature phase (cf. Fig. 2d and a for comparison). The predicted single line can now be observed at δ_{iso} = −156.8 ppm after a decoupling of ^{115}In. It has a width of 0.34 kHz (Fig. 2e). In the cubic phase the broad species (Fig. 2d) is obviously caused by the fluorine–indium scalar coupling. The latter is strongly supported and evidenced by the direct observation of the scalar In–F coupling in the ^{115}In MAS NMR spectrum as depicted in Fig. 3B. The shape of the spectrum with 7 lines in the binomial intensity ratio (Fig. 3B) proves the existence of isolated symmetric (InF_6) units with 6 equivalent fluorine ligands in the cubic phase. A scalar coupling constant of J = 284 Hz was determined by simulation at an isotropic chemical shift value of −122 ppm for ^{115}In. Fluorine decoupling gives a single narrow signal of ^{115}In which is rarely observable and finally only in a high symmetric (cubic) phase (FWHM: 0.2 kHz). However, the scalar coupling alone does not satisfyingly explain the line shape of the ^{19}F signal shown in Fig. 2d. A reconstruction of this spectrum is possible if in addition to the species with scalar coupling two small contributions are added in its low- and high-field parts. The respective parameters are summarized in Table 3.

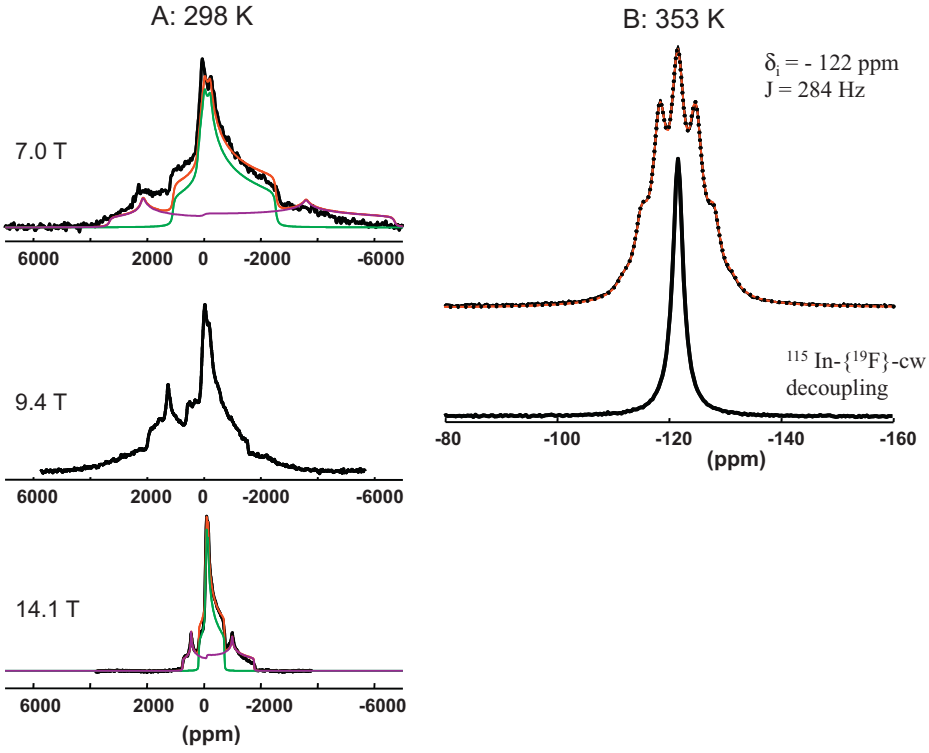

Fig. 3. Static (A) and MAS (B) (ν_{rot} = 25 kHz) ^{115}In NMR spectra of $(NH_4)_3InF_6$ together with their deconvolution (parameters of deconvolution are given in Table 2).

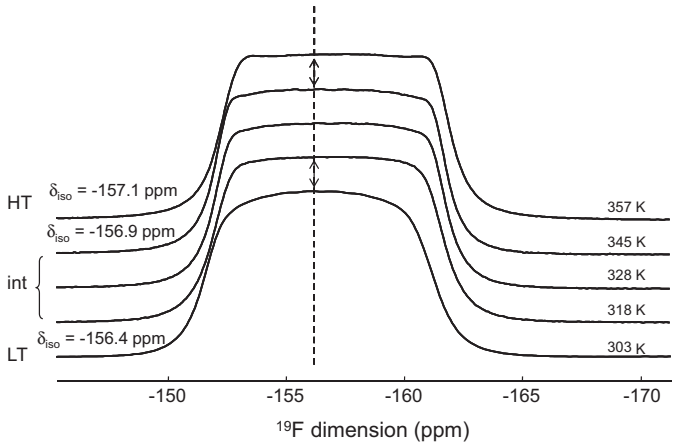

Fig. 4. ^{19}F MAS NMR spectra of $(NH_4)_3InF_6$ recorded at 7 T versus temperature following the reversible phase transition in situ. The different phases are indicated as in Fig. 1.

In addition to the experiments at room temperature and at 353 K the reversible phase transition of $(NH_4)_3InF_6$ was followed in dependence on the temperature by ^{19}F MAS NMR in situ (Fig. 4). With increasing temperature a first shift of the centre of gravity of the line towards lower δ_{iso} values can be observed between 303 K and 318 K, corresponding to the transition between the room-temperature and 'intermediate' phases. A second shift is observed between 345 K and 357 K, corresponding to the transition to the cubic phase of $(NH_4)_3InF_6$. One can notice that the lines at lower temperatures are broader, preventing the resolution of the *J* pattern, and change with increasing temperature their shape, width and position.

Meanwhile it is well known that fast spinning leads to a local heating of the solid sample. Therefore MAS experiments were performed with a rotation frequency of 34 kHz and a bearing gas temperature of 298 K, i.e. without additional external heating. Grimmer et al. [16] performed a calibration of the sample temperature under fast MAS conditions with the ^{119}Sn signal of the chemical shift thermometer $Sm_2Sn_2O_7$. Following this calibration [16] the temperature which can be expected for the sample at a spinning frequency of 34 kHz is 332 K, i.e. above room temperature but still 20 K below the known phase transition temperature. The corresponding ^{19}F MAS NMR spectra are shown in Fig. 2c together with a deconvolution. Four contributions are necessary for this decomposition consisting of a line at −156.5 ppm with scalar coupling (84%), a broad line at the same position (14%) and two lines of low intensity (1% each) in the low- and high-field parts of the spectrum (−153.3 ppm, −159.7 ppm). The line widths of the latter three lines are very similar to those obtained for the cubic phase with 25 kHz spinning speed. In the Indium spectrum no signal was detectable (not shown here).

Table 4
Cell parameters of the diffractograms shown in Fig. 5.

Structure	Symmetry	Parameters
(A)	Tetragonal	$a = 6.5020(13)$ Å, $c = 9.4672(23)$ Å
(B)	Monoclinic	$a = 6.5019(49)$ Å, $b = 9.4928(38)$ Å, $c = 9.4598(23)$ Å, $\beta = 90.24(4)^\circ$

2.3. $(NH_4)_3InF_6$ – X-ray diffraction

The X-ray diffractogram of $(NH_4)_3InF_6$ at room temperature interestingly varies over the sample. Spatial resolution gives two different diffractograms, which are shown in Fig. 5. Cell parameters were extracted by LeBail fit (Table 4). Rietveld solution of the structure was not possible.

3. Discussion

The different space groups determined for the room temperature and high-temperature cubic phases of $(NH_4)InF_6$ cause dramatic consequences for the observed NMR spectra of both probe nuclei. ^{19}F MAS NMR experiments resulted in unusual line shapes of the room temperature spectra (Fig. 2a and c). In the MAS NMR spectra the resolution of different fluorine sites is prevented by the action of residual homo- and heteronuclear dipolar couplings, possible effects of ^{19}F chemical shift anisotropies as well as especially the presence of scalar coupling. An estimation of the order of magnitude results in a comparable range for dipolar interactions (F–F: ∼10 kHz, F–H: ∼12 kHz), and ^{19}F chemical shift anisotropy (∼10 kHz at 7 T). It can be assumed that the loss of mobility of the octahedra at lower temperatures is responsible for a reduced averaging of the F–F dipolar interaction under MAS.

At 353 K it seems that small amounts of the fluorine sites, obviously present at lower temperature, are still observable. However, the main contribution arises from the typical fluorine site of the cubic phase at −156.8 ppm (Table 3). All ^{19}F MAS NMR spectra (Fig. 2a, c and d) recorded without ^{115}In decoupling show a symmetric shape. Therefore, in $(NH_4)_3InF_6$ possible residual dipolar couplings between the spin-1/2 (^{19}F) and the quadrupolar nucleus (^{115}In) must be negligible. The latter can be explained with the high symmetry of local $(InF_6)^{3-}$ units which is in contrast to a situation observed for K_2NbF_7 [17]. If present, it would be manifested

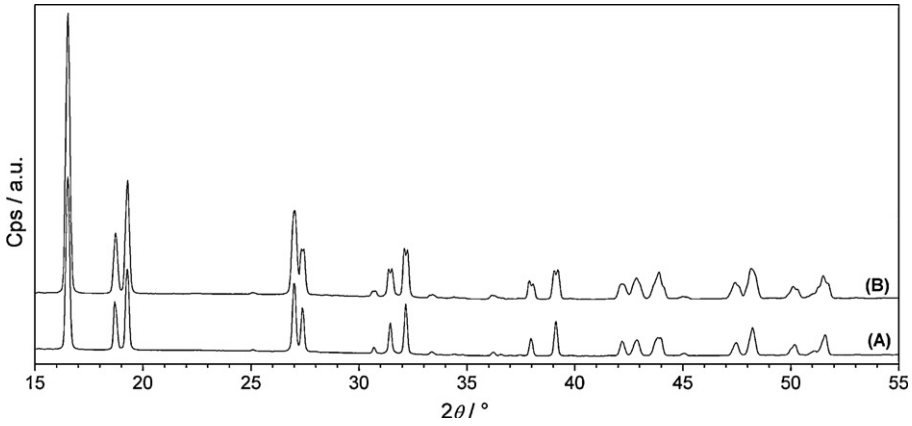

Fig. 5. Cutout of the X-ray diffractograms of $(NH_4)_3InF_6$ at room temperature. (A) and (B) indicate different spots inside the sample.

in increasing or decreasing spacing between peaks in the multiplet and a less symmetric line shape, not observed here (Fig. 2c).

A narrow signal of one ^{115}In site at −122 ppm is observed in the cubic phase as well, which is very scarce in the literature. Moreover, the existence of isolated InF_6 octahedra in the cubic phase is directly proven by MAS NMR due to the resolved scalar coupling (Fig. 3B).

The resolution and assignment of Indium sites at room temperature are much more complicated. So far, the simulation of the static ^{115}In NMR spectra (Fig. 3A) is in acceptable agreement with the spectra recorded at 7 and 14 T, and was achieved using two indium sites of close relative intensity and an isotropic chemical shift value similar to that of the cubic phase (−122 ppm) (Table 2). Chemical shift anisotropies are very small and do not noticeably affect the determined parameters. Deviations in the low-field part of the spectrum taken at 9.4 T are most likely due to background signals of the probe, since the measurements at the different static magnetic fields were carried out on the same sample. In addition, as confirmed by space-resolved synchrotron X-ray powder diffraction measurements, the sample is not completely phase pure (Fig. 5). Obviously, the phase transition between the monoclinic and tetragonal phases is induced very easily, but does not proceed completely. Thus it was impossible to obtain phase-pure samples. Therefore, the two Indium signals observed on the room temperature ^{115}In NMR spectrum can be tentatively assigned to one or the other phase. Since they have close relative intensity, this would indicate a balanced mixture of both phases in the studied room temperature sample.

The observed scalar coupling $J(^{19}F–^{115}In) = 284$ Hz is in the same range as observed for the related compound $(NH_4)_3GaF_6$ ($J(^{19}F–^{71}Ga) = 264$ Hz, $J(^{19}F–^{69}Ga) = 197$ Hz) [12].

A comparison of Fig. 2a–d shows that ^{19}F MAS NMR indicates not only differences between the room temperature and high temperature phases, but also changes within the phase transition. The latter is supported by ^{115}In MAS NMR (not shown here). Neither broad lines nor the expected unclear multi-line spectrum of ^{115}In can be recorded applying a rotation frequency of 34 kHz. A detection of an indium signal is not possible, which is a typical appearance of the behaviour of spin probes within phase transitions.

4. Conclusion

Solid state NMR was applied to study the room and high temperature phases of $(NH_4)_3InF_6$ using ^{19}F and ^{115}In as probe nuclei. For the first time static ^{115}In spectra of $(NH_4)_3InF_6$ were taken at three different fields at room temperature. Their reconstruction was possible in an acceptable manner with two different In sites. One fluorine site was unambiguously observed in the cubic phase. In the room temperature phase scalar couplings and residual dipolar couplings prevent a determination of the number of fluorine sites. At higher temperatures both NH_4 groups and InF_6 groups undergo rapid reorientation rotations and as a consequence the ^{19}F lines are motionally narrowed and the line shape is dominated by the scalar coupling. The scalar In–F coupling in the cubic phase is directly observable with $J = 284$ Hz, larger than for the related gallium compound.

The occurrence of two different In sites agrees with the occurrence of the different phases, namely the tetragonal and the monoclinic ones.

5. Experimental

5.1. Synthesis

A solution of 3.69 g of $In(NO_3)_3{\cdot}5H_2O$ in 20 mL of water was added to a solution of 5.20 g of NH_4F (F/In ratio >14) in 10 mL of water under vigorous stirring within 30 min. After further stirring overnight, a white precipitate of $(NH_4)_3InF_6$ occurred, which was filtered off, washed with water and ethanol, and dried at 120 °C. Neither FTIR nor ^{1}H MAS NMR shows evidence of OH groups in the solid being substituted for fluorine.

5.2. Solid state NMR

^{19}F and ^{115}In MAS NMR spectra were recorded on a Bruker AVANCE 400 spectrometer (Larmor frequencies: $\nu_{^{19}F} = 376.4$ MHz, $\nu_{^{115}In} = 87.7$ MHz) using a 2.5 mm probe (Bruker Biospin) and applying spinning speeds up to 34 kHz.

^{19}F MAS NMR ($I = 1/2$) spectra were recorded with a $\pi/2$ pulse duration of p1 = 3.7 μs, a spectrum width of 400 kHz, a recycle delay of 5 s and an accumulation number of 16. Existent background signals of ^{19}F were suppressed with the application of a phase-cycled depth pulse sequence according to Cory and Ritchey [18] and a rotor synchronized echo pulse sequence.

^{115}In MAS NMR ($I = 9/2$) spectra were taken with a single pulse duration of 1 μs, a recycle delay of 0.5 s, a sweep width of 500 kHz and 5000 accumulations. The variable temperature ^{19}F MAS NMR Hahn-echo spectra were recorded on an Avance 300 Bruker NMR spectrometer (Larmor frequency of 282.2 MHz). The sample temperature was calibrated using the ^{207}Pb isotropic chemical shift of $Pb(NO_3)_2$ as NMR thermometer [19,20].

Static ^{115}In NMR experiments were performed with a 4 mm probe at Bruker Avance 300, 400 and 600 spectrometers (Larmor frequencies: $\nu_{^{115}In} = 65.7$ MHz, 87.7 MHz and 131.5 MHz, respectively). Accumulation numbers up to 108,000 and recycle delays of 1 s were chosen for an optimal signal to noise ratio.

The isotropic chemical shifts δ_{iso} of ^{19}F and ^{115}In resonances are given with respect to $CFCl_3$ standard and a 0.1 M solution of $In(NO_3)_3$, respectively.

All spectra were simulated using dmfit-program package (version 2008) [21].

5.3. XRD

X-ray diffraction experiments were performed at the synchrotron micro focus beamline μSpot (BESSY II of the Helmholtz Centre Berlin for Materials and Energy) with a rotation capillary equipment ($\lambda = 0.82656$ Å, beam∅ = 20–100 μm). Scattered intensities were collected 200 mm behind the sample position with a two-dimensional X-ray detector. The obtained scattering images were processed and converted into diagrams of scattered intensities versus scattering vector q ($q = 4\pi/\lambda \sin\theta$). The wave length was recalculated to Cu $K_{\alpha 1}$.

Acknowledgements

Dr. M. Body (Le Mans) and Dr. F. Emmerling (BAM, Berlin) are kindly acknowledged for support and performing the X-ray powder diffraction measurements, respectively.

References

[1] I.N. Flerov, M.V. Gorev, K.S. Aleksandrov, A. Tressaud, J. Grannec, M. Couzi, Mater. Sci. Eng. 24 (1998) 81–151.
[2] K. Moriya, T. Matsuo, H. Suga, S. Seki, Bull. Chem. Soc. Jpn. 50 (1977) 1920–1926.
[3] K. Moriya, T. Matsuo, H. Suga, S. Seki, Bull. Chem. Soc. Jpn. 52 (1979) 3152–3162.
[4] A. Tressaud, S. Khairoun, L. Rabardel, T. Kobayashi, T. Matsuo, H. Suga, Phys. Status Solidi A 96 (1986) 407–414.
[5] I.N. Flerov, M.V. Gorev, J. Grannec, A. Tressaud, J. Fluorine Chem. 116 (2002) 9–14.
[6] M.V. Gorev, I.N. Flerov, A. Tressaud, J. Phys.: Condens. Matter 11 (1999) 7493–7500.
[7] H. Bode, E. Voss, Z. Anorg. Allg. Chem. 290 (1957) 1–16.
[8] S. Schwarzmann, Fortschr. Miner. 42 (1966) 231.
[9] R.A. Vecher, L.M. Volodkovich, G.S. Petrov, A.A. Vecher, Thermochim. Acta 87 (1985) 377–380.

[10] A.C.A. Jayasundera, R.J. Goff, Y. Li, A.A. Finch, P. Lightfoot, J. Solid State Chem. 183 (2010) 356–360.
[11] N. Böhmer, G. Meyer, Z. Anorg. Allg. Chem. 627 (2001) 1248–1252.
[12] T. Krahl, M. Ahrens, G. Scholz, D. Heidemann, E. Kemnitz, Inorg. Chem. 47 (2008) 663–670.
[13] K. Yamada, K. Kumano, T. Okuda, Solid State Ionics 176 (2005) 823–829.
[14] K. Yamada, K. Kumano, T. Okuda, Solid State Ionics 177 (2006) 1691–1695.
[15] F. Chen, G.B. Ma, R.G. Cavell, V.V. Terskikh, R.E. Wasylishen, Chem. Commun. (2008) 5933–5935.
[16] B. Langer, L. Schnell, H.W. Spiess, A.R. Grimmer, J. Magnet. Reson. 138 (1999) 182–186.
[17] L.S. Du, R.W. Schurko, K.H. Lim, C.P. Grey, J. Phys. Chem. A 105 (2001) 760–768.
[18] D.G. Cory, W.M. Ritchey, J. Magn. Reson. 80 (1988) 128–132.
[19] L.C.M. van Gorkom, J.M. Hook, M.B. Logan, J.V. Hanna, R.E. Wasylishen, Magn. Reson. Chem. 33 (1995) 791–795.
[20] A. Bielecki, D.P. Burum, J. Magn. Reson. 116 (1995) 215–220.
[21] D. Massiot, F. Fayon, M. Capron, I. King, S. Le Calve, B. Alonso, J.O. Durand, B. Bujoli, Z.H. Gan, G. Hoatson, Magn. Reson. Chem. 40 (2002) 70–76.